ESMO GOOD SCIENCE BETTER MEDICINE BEST PRACTICE

ANNALS OF ONCOLOGY driving innovation in oncology

ORIGINAL ARTICLE

Genome-wide profiling of non-smoking-related lung cancer cells reveals common *RB1* rearrangements associated with histopathologic transformation in *EGFR*-mutant tumors

E. Pros[1], M. Saigi[1,2], D. Alameda[3], G. Gomez-Mariano[4], B. Martinez-Delgado[4], J. J. Alburquerque-Bejar[1], J. Carretero[5], R. Tonda[6], A. Esteve-Codina[6], I. Catala[7], R. Palmero[2], M. Jove[2], C. Lazaro[8,9], A. Patiño-Garcia[3], I. Gil-Bazo[3,9], S. Verdura[1], A. Teulé[8,9], J. Torres-Lanzas[10], D. Sidransky[11], N. Reguart[12,13], R. Pio[3,9], O. Juan-Vidal[14], E. Nadal[2,15], E. Felip[16], L. M. Montuenga[3,9,17] & M. Sanchez-Cespedes[1*†]

[1]Genes and Cancer Group, Cancer Epigenetics and Biology Program (PEBC), Bellvitge Biomedical Research Institute (IDIBELL), Hospitalet de Llobregat, Barcelona; [2]Department of Medical Oncology, Catalan Institute of Oncology (ICO), Hospitalet de Llobregat, Barcelona; [3]Program in Solid Tumors, Center for Applied Medical Research (CIMA), University of Navarra and Navarra Health Research Institute (IDISNA), Pamplona; [4]Molecular Genetics Unit, Rare Diseases Institute of Research (IIER), Health Institute Carlos III, Majadahonda, Madrid; [5]Department of Physiology, Faculty of Medicine and Odontology, University of Valencia, Valencia; [6]CNAG-CRG, Centre for Genomic Regulation (CRG), Institute of Science and Technology (BIST) and University Pompeu Fabra (UPF), Barcelona; [7]Pathology Department, Bellvitge University Hospital, Hospitalet de Llobregat; [8]Hereditary Cancer Program, Catalan Institute of Oncology, ICO-Oncobell-IDIBELL, Madrid; [9]CIBERONC, Health Institute Carlos III, Madrid; [10]Thoracic Surgery Department, Hospital Universitario Virgen de la Arrixaca, El Palmar-Murcia, Spain; [11]Department of Otolaryngology and Head and Neck Surgery, Johns Hopkins University, School of Medicine, Baltimore, Maryland; [12]Oncology Department, Thoracic Tumors Unit, Clinic Hospital; [13]Translational Genomics and Targeted Therapeutics in Solid Tumors, August Pi i Sunyer Biomedical Research Institute (IDIBAPS), Barcelona; [14]Biomarkers and Precision Medicine Unit, Research Institute La Fe and Department of Medical Oncology, La Fe University Hospital, Valencia; [15]Clinical Research in Solid Tumors Group (CReST), Oncobell Program, Bellvitge Biomedical Research Institute (IDIBELL), Hospitalet de Llobregat; [16]Oncology Department, Vall d'Hebron University Hospital and Vall d'Hebron Institute of Oncology, Barcelona; [17]Department of Pathology, Anatomy and Physiology, Schools of Medicine and Sciences, University of Navarra, Pamplona, Spain

Available online 6 January 2020

Background: The etiology and the molecular basis of lung adenocarcinomas (LuADs) in nonsmokers are currently unknown. Furthermore, the scarcity of available primary cultures continues to hamper our biological understanding of non-smoking-related lung adenocarcinomas (NSK-LuADs).

Patients and methods: We established patient-derived cancer cell (PDC) cultures from metastatic NSK-LuADs, including two pairs of matched *EGFR*-mutant PDCs before and after resistance to tyrosine kinase inhibitors (TKIs), and then performed whole-exome and RNA sequencing to delineate their genomic architecture. For validation, we analyzed independent cohorts of primary LuADs.

Results: In addition to known non-smoker-associated alterations (e.g. *RET, ALK, EGFR,* and *ERBB2*), we discovered novel fusions and recurrently mutated genes, including *ATF7IP,* a regulator of gene expression, that was inactivated in 5% of primary LuAD cases. We also found germline mutations at dominant familiar-cancer genes, highlighting the importance of genetic predisposition in the origin of a subset of NSK-LuADs. Furthermore, there was an over-representation of inactivating alterations at *RB1*, mostly through complex intragenic rearrangements, in treatment-naive *EGFR*-mutant LuADs. Three *EGFR*-mutant and one *EGFR*-wild-type tumors acquired resistance to EGFR-TKIs and chemotherapy, respectively, and histology on re-biopsies revealed the development of small-cell lung cancer/squamous cell carcinoma (SCLC/LuSCC) transformation. These features were consistent with *RB1* inactivation and acquired *EGFR-T790M* mutation or *FGFR3—TACC3* fusion in *EGFR*-mutant tumors.

Conclusions: We found recurrent alterations in LuADs that deserve further exploration. Our work also demonstrates that a subset of NSK-LuADs arises within cancer-predisposition syndromes. The preferential occurrence of *RB1* inactivation, via complex rearrangements, found in *EGFR*-mutant tumors appears to favor SCLC/LuSCC transformation under growth-inhibition pressures. Thus *RB1* inactivation may predict the risk of LuAD transformation to a more aggressive type of lung cancer, and may need to be considered as a part of the clinical management of NSK-LuADs patients.

Key words: nonsmokers, lung adenocarcinoma, *EGFR*, *RB1*, tyrosine kinase inhibitors, whole-exome sequencing

INTRODUCTION

Lung cancer (LC) is the primary cause of death from cancer in most Western countries,[1] with adenocarcinomas (LuADs), squamous cell carcinomas (LuSCCs), and small-cell lung cancer (SCLC) the most commonly diagnosed types. Although tobacco smoking is the main risk factor for LC, 10%—20% of LuAD cases will arise in nonsmokers.[2] LC among nonsmokers is significantly more common in women than men,[2] and has some

*Correspondence to: Dr Montse Sanchez-Cespedes, Genes and Cancer Group, Cancer Epigenetics and Biology Program (PEBC), Bellvitge Biomedical Research Institute (IDIBELL), Hospital Duran i Reynals, 3a planta - Gran Via de Hospitalet, 199, 08908 Hospitalet de Llobregat, Barcelona, Spain

E-mail: mscespedes@carrerasresearch.org (M. Sanchez-Cespedes).

†Current address: Cancer Genetics Group, Josep Carreras Leukaemia Research Institute-IJC Building, Campus ICO-Germans Trias i Pujol, Cancer Genetics Group, Carretera de Can Ruti, Camí de les Escoles s/n, 08916 Badalona, Barcelona, Spain. Tel: +34-93-557-28-00 (ext. 4260)

distinctive gene alteration features, including a lower mutational burden and activating gene alterations at growth factor receptors, for example, ALK, EGFR, ERBB2, ROS1, and RET, that do not coexist.[3,4] The presence of these mutations confers therapeutic benefits because these molecules are amenable to inhibition by specific tyrosine kinase inhibitors (TKIs).[5] By contrast, LuADs in smokers have a different gene alteration profile with simultaneous alterations in several known cancer genes (e.g. *KRAS*, *STK11*) and are more likely to have a greater mutational burden.[4,6] The few genome-wide studies of LuADs from nonsmokers have focused on *EGFR*-mutant tumors and have yielded promising information about the underlying genetics of these tumors, including concurrent mutations of potential biological relevance.[7,8]

Studies of cancer cell lines have been responsible for some major contributions to our understanding of LC biology and pathogenesis as well as providing useful tools for translational research.[9,10] Cultured tumor cells, which accurately represent tumor cells *in vivo*, are basically populations of pure tumor cells without admixed stromal or inflammatory cells that can mask the mutations present in the tumor cells.[9] Although >250 LC cell lines from all histopathological subtypes are available, there are very few derived from nonsmoker LuAD patients, which has limited our understanding of the biology of these tumors. Thus a larger set of LC cell lines with these characteristics is required if we are to gain a deeper understanding of the molecular basis of lung carcinogenesis in nonsmoker individuals and be able to analyze the mechanisms that drive resistance to TKIs.

Here, we have established a repertoire of patient-derived cancer cell (PDC) cultures from non-smoking-related LC patients and performed an integrated genomic (i.e. somatic and germline gene alterations and expression profile) and molecular analysis.

PATIENTS AND METHODS

Tumor samples and generation of LC cell cultures

PDC cultures ($n = 13$) were established from the malignant pleural effusions of 11 different LuAD patients, from the Catalan Institute of Oncology (supplementary Table S1, available at *Annals of Oncology* online). Cancer cells were isolated as previously described (supplementary methods, available at *Annals of Oncology* online).[10] Validation cohorts consisted, in most cases, in tumor specimens collected at the time of surgery (stage I—III tumors) or from diagnostic biopsies (supplementary Figure S1A, supplementary Table S2, and supplementary methods, available at *Annals of Oncology* online). Normal DNA was obtained from blood or adjacent normal tissue. Written consent was obtained and procedures were approved by the Institutional Review Board of Institut d'Investigacio Biomedica de Bellvitge (IDIBELL).

Whole-exome sequencing, RNA sequencing, and data analysis

Whole-exome sequencing (WES), RNA-seq, and data analysis were carried out at the Spanish National Genome Analysis Center (CNAG, Barcelona, Spain; supplementary methods and supplementary Table S3, available at *Annals of Oncology* online).[11]

Multiplex ligation-dependent probe amplification and RB1 panel for mutational screenings

Multiplex ligation-dependent probe amplification was used to test for complex rearrangements at *RB1*. For the mutational analysis a custom-designed *RB1* panel was used (http://sequencing.roche.com/products/software/nimbledesign-software.html; supplementary methods, available at *Annals of Oncology* online).

Statistical analysis

Analysis consisted of chi-square, two-tailed unpaired Student's *t*-test, Mann—Whitney test, and analysis of variance, as appropriate. Continuous variables are summarized as means and standard deviations.

RESULTS

Establishment of a PDC repertoire from non-smoking-associated LCs and assessment of genome-wide characteristics

We established PDCs cultures from the discarded pleural liquid drained from 11 non-smoking-related lung adenocarcinoma (NSK-LuAD) patients (supplementary Table S1 and supplementary Figure S1B, available at *Annals of Oncology* online). NSK-LuADs were defined as those adenocarcinomas of the lung that fulfilled at least one of the following conditions: (i) occur in a never-smoker or >25-year ex-smoker, (ii) bear *EGFR* or *ALK* alterations, or (iii) arise in individuals ≤48 years of age. The features of the patients and tumors including prior knowledge of the genetics of the tumors are described in supplementary Table S1 (available at *Annals of Oncology* online).

We performed WES and RNA-seq and found a mutation frequency in coding regions that ranged from 76 to 499 across the PDCs (Figure 1A). The only current smoker, despite being relatively young (46 years), developed the tumor with the highest mutation frequency ($n = 499$). The relative frequency of C:G>A:T transversions in the PDCs was relatively low (<20%) and similar to that reported for LuAD in nonsmokers.[3] Following pre-established criteria (supplementary Figure S2A, available at *Annals of Oncology* online), we selected the genes affected by somatic non-silent alterations (supplementary Tables S4—S6, available at *Annals of Oncology* online). Genetic activation was found at several known oncogenes, including high-level amplification involving *MDM2,* whereas tumor-suppressor genes (TSGs) exhibited biallelic inactivation, such as *TP53* and *RB1* (Figure 1A). Alterations at *RB1* were through homozygous deletions and appeared in the three *EGFR*-mutant PDCs. The PDC10 did not express *TP53* and a detailed analysis revealed the presence of a *TP53/FXN* transcript, which confirmed a complex mechanism of *TP53* inactivation (supplementary Figure S2B, available at *Annals of Oncology* online).

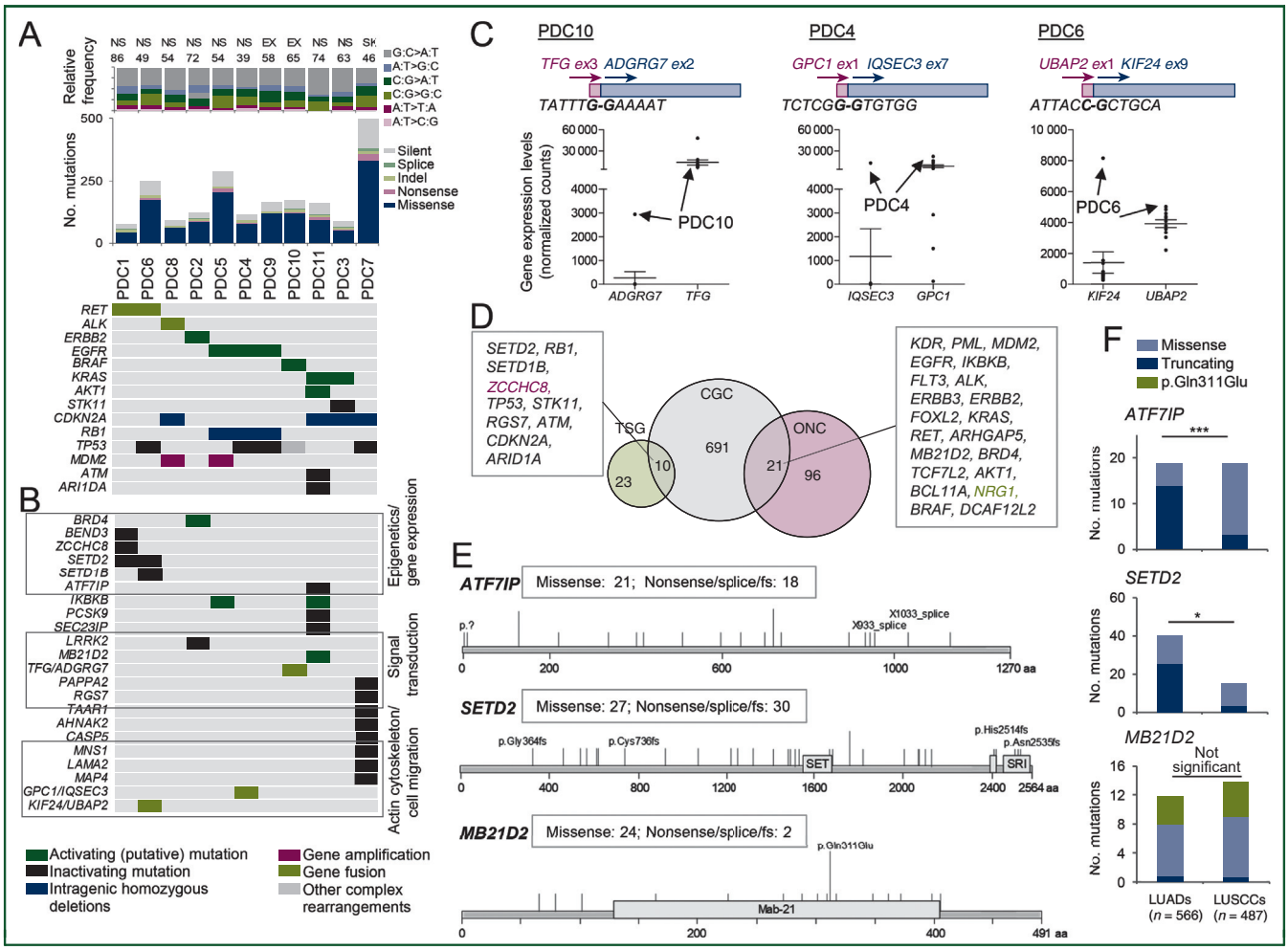

Figure 1. Somatic gene alterations detected by whole-exome sequencing (WES) and RNA-seq analysis of the non-smoking-related lung adenocarcinoma (NSK-LuAD) cells. (A) Top panel, histograms display the type of base-pair substitution and the exonic mutation burden (nonsynonymous, nonsense, splicing, and indel mutations) from the WES analysis referred to each sequenced patient-derived cancer cells (PDCs). Bottom panel, oncoplot depicting the alterations, in well-established cancer genes, in the indicated lung cancer cell lines. (B) Selection of candidate tumor-suppressor genes (TSGs) and oncogenes (ONCs; from supplementary Table S7, available at *Annals of Oncology* online) and the related functions involved, as indicated. (C) Top panel, identification, by RNA-seq, of three in-frame fusion transcripts in the indicated cells. Bottom panel, representation of the gene expression levels of each of the genes involved in the fusions, in all the PDCs from the current study. (D) Venn diagram indicates the TSGs and ONCs from the current study that overlap the Cancer Gene Census (CGC), available in the COSMIC database (list of overlapping genes included in the two squares). *ZCCHC8* is a TSG candidate that is listed as an ONC in the CGC and *NRG1* is an ONC candidate that is listed as a TSG in the CGC. (E) Schematic representation of ATF7IP, SETD2, and MB21B2 proteins and location of the inactivating mutations (for *ATF7IP* and *SETD2*) and of the point mutations (for *MB21D2*) found in our cohorts of LuADs (PDCs and primaries; $n = 33$) and in two TCGA cohorts (http://www.cbioportal.org/). The mutations detailed are from the current work. (F) Distribution of the missense and truncating mutations, for each indicated gene, in the LuAD and lung squamous cell carcinoma (LuSCC) cohorts from TCGA. *P <0.05; ***P <0.005.

EX, ex-smoker; NS, nonsmoker; SK, current smoker; TCGA, The Cancer Genome Atlas.

Recurrent mutations and novel fusions in LuADs

Following an established criterion[11] we filtered our candidates (from supplementary Tables S4—S6, available at *Annals of Oncology* online) to search for additional oncogenes and TSGs. The analysis yielded 27 TSG and 109 oncogene candidates that coded for proteins involved in different functions (Figure 1B and supplementary Table S7, available at *Annals of Oncology* online). The candidates include three fusions with one of the partners overtly overexpressed (Figure 1C). Overexpression of these genes was confirmed in LCs from The Cancer Genome Atlas (TCGA) database (supplementary Figure S3, available at *Annals of Oncology* online). The *TFG—ADGRG7* fusion was also in the DNA from the blood, as previously reported.[12]

Next, we compared our selected candidates (supplementary Table S7, available at *Annals of Oncology* online) and the *bona fide* TGS and oncogenes with the COSMIC-Cancer Gene Census (CGC).[13] One-third of the TSGs and one-fifth of the oncogenes found in this study were present in the CGC (Figure 1D).

To determine whether the mutations in the candidates were recurrent, we scrutinized the WES data in the independent cohort of stages I—III primary NSK-LuADs (supplementary Table S2 and supplementary Figure S1A, available at *Annals of Oncology* online). We found inactivating alterations at *ATF7IP*, *GBP3*, *SETD1B,* and *SETD2*; the latter two were in the CGC. The recorded nonsynonymous mutations at the *SETD2* and *ATF7IP* genes in the TCGA were >5% for non-small-cell lung cancer, half of which are listed

as truncating (Figure 1E). This is above the threshold (>20%) proposed for TSG candidates.[14] Inactivating mutations at these genes were more common in LuADs than in LuSCCs (Figure 1F), although we could not conclude a predominance in nonsmokers (data not shown). Finally, a heterozygous change, p.Gln311Glu, at *MB21D2* found at PDC11 was found in 1% of the LuADs and LuSCCs of the TCGA (Figure 1E and F). The mutation affects a conserved amino acid within the Mab-21 domain (supplementary Figure S4, available at *Annals of Oncology* online). The change appeared at similar frequencies in head and neck squamous cell carcinomas and in bladder urothelial carcinomas, but not in other common cancers.

RB1 inactivation by intragenic complex rearrangements predominates in *EGFR*-mutant LuADs

The three *EGFR*-mutant PDCs presented inactivation of *RB1*, all by deletions involving one or more exons. Although a selective presence of *RB1* mutations in LuADs from *EGFR*-mutant tumors has been observed,[9,15] the intragenic complex rearrangements (ICRs) have not been examined. Here, we scrutinized an independent cohort of LuADs for mutations and ICRs at *RB1* (supplementary Table S2, available at *Annals of Oncology* online). Alterations at *RB1* were found in seven (14%) of the tumors analyzed, six of which consisted of ICRs (Figure 2A and B). The frequency of *RB1* inactivation was significantly higher in the *EGFR*-mutant (41%) than in the *EGFR*-wild-type (1%) tumors. The former rate is similar to that reported for the cohort of SCLC cell lines from the Cancer Cell Line Encyclopedia database. However, whereas in SCLC *RB1* was inactivated mostly through point mutations, it was preferentially achieved via ICR in *EGFR*-mutant LuADs (Figure 2C).

SCLC and LuSCC transformation in *RB1*-inactivated LuADs

One *EGFR*-mutant/*RB1*-inactivated tumor (patient #4) switched from LuAD to mixed SCLC/LuSCC at clinical progression to EGFR-TKI, which prompted us to look for additional LuADs that had transformed to SCLC/LuSCC.

Patient #4 was diagnosed with an *EGFRex19*-mutant LuAD with lung, pleural, and brain metastasis. A malignant pleural effusion was obtained before afatinib treatment and PDC4 was derived. After an initial partial response, she developed brain and lung progression (Figure 3A). The genotyping of a liquid biopsy discarded the *EGFR-T790M* mutation and carboplatin—pemetrexed treatment was administered, achieving a remarkable shrinkage of the lung lesion but an enlargement of a mediastinal lymph node. A pleural biopsy after relapse revealed LuSCC morphology and a biopsy from the lymph node showed combined SCLC/LuSCC features and the ICR at *RB1* (Figure 3B and C).

Patient #76, diagnosed with an *EGFRex19*-mutant LuAD and bone metastasis, underwent treatment with dacomitinib, showing a partial response. At progression, the *EGFR-T790M* mutation was detected in a liquid biopsy and the patient was treated with osimertinib. After the patient progressed with new bone/liver metastasis, the analysis of multiple genes in a liquid biopsy identified an *RB1* mutation (p.Leu683fs),

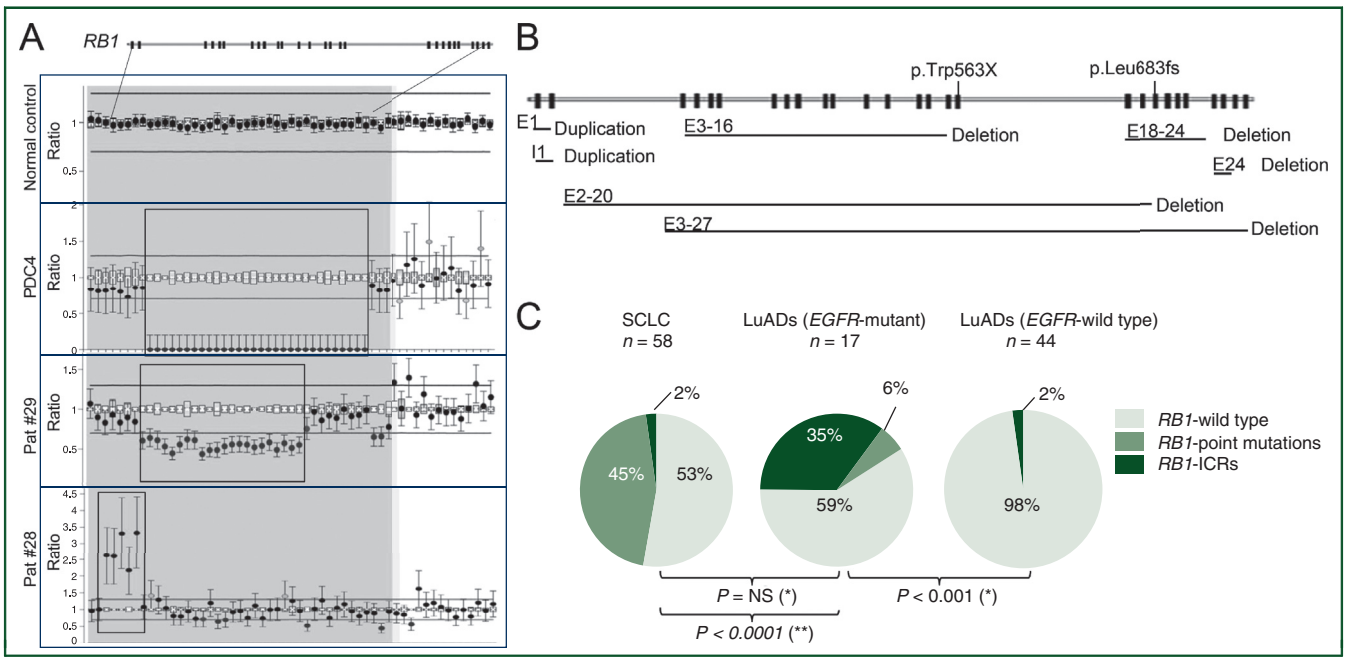

Figure 2. ***RB1*** **is preferentially inactivated, mostly by intragenic complex rearrangements (ICRs), in** ***EGFR*****-mutant LuADs. (A) Upper panel, schematic representation of the structure of** ***RB1,*** **with all its corresponding exons. Bottom panels, ratio charts of the multiplex ligation-dependent probe amplification (MLPA) depicting the intragenic deletions of various exons in two tumors and the duplication of intron 1 in one of the tumors. An appropriate normal control is also included. The black rectangles indicate the exons that had experienced intragenic homozygous deletion or duplications. (B) Schematic representation of the** ***RB1*** **structure to show the spanning point mutations (above) and the ICR (lines below) found in the screening. (C) Pie charts comparing the frequency of** ***RB1*** **alterations in the three groups of lung cancers (single asterisk) or the type of** ***RB1*** **alterations among small-cell lung cancer cells (from Cancer Cell Line Encyclopedia) and** ***EGFR*****-mutant LuADs (double asterisk) (supplementary Figure S1A, available at** ***Annals of Oncology*** **online).**
E, exon; I, intron; LuAD, lung squamous cell carcinoma; NS, not significant.

confirmed by Sanger sequencing (supplementary Figure S5A, available at *Annals of Oncology* online), but not the *EGFR-T790M*. A liver biopsy showed the same genotype along with SCLC morphology (Figure 3A).

Patient #59 was diagnosed with locally advanced, *EGFR*-wild-type LuAD and underwent concurrent chemo-radiotherapy. After 32 months, the disease progressed to the brain and she underwent surgery and focal radiotherapy. The metastatic lesion exhibited LuSCC features (TTF1/CK7/CK20-positive immunostaining). Five months later, after lymph-node progression, a biopsy showed a mixed SCLC/LuSCC and a duplication of various exons at *RB1* (Figure 3C). The patient received platinum-based chemotherapy but developed bone metastasis, which showed LuSCC features. There was no DNA left from the original primary tumor to determine the baseline status of *RB1* in patients #76 and #59.

Finally, patient #5 was diagnosed with an *EGFRex19*-positive LuAD with multiple metastases. Nine months after treatment with gefitinib, the disease progressed and the analysis of liquid and pleural biopsies showed LuAD features but not *EGFR-T790M* mutation. After treatment with afatinib, the disease rapidly progressed and no additional biopsies were taken (Figure 3A). Two PDCs were derived from this patient: after diagnosis at 8 months (PDC5) and at 11 months (PDC5.2), following progression to afatinib. Both PDCs carried identical alteration at *RB1*, and PDC5.2 showed SCLC/LuSCC characteristics and an *FGFR3—TACC3* fusion (details in the following section).

Acquired resistance to EGFR-TKI shows evidence of combined SCLC and LuSCC features and additional gene alterations

The PDC4.2 and PDC5.2, derived after the patients progressed to EGFR-TKIs, had acquired changes in morphology (Figure 4A). In cell culture, the PDC5.2 samples were less sensitive to erlotinib and afatinib than the pretreatment counterpart (Figure 4B and supplementary Figure S5B, available at *Annals of Oncology* online). Despite reduced EGFR levels, both cells maintained the ability to decrease pEGFR and block extracellular receptor kinase phosphorylation upon treatment (Figure 4C and D and supplementary Figure S5C, available at *Annals of Oncology* online). Thus the acquired resistance to the TKI in these cells does not involve changes in EGFR activity. To study the molecular mechanisms underlying resistance to the TKIs in these tumors, we performed WES and RNA-seq on PDC4.2 and PDC5.2 and compared them with their pretreated counterparts. WES confirmed the *EGFR* mutations and the ICRs at *RB1* and RNA-seq yielded evidence of overexpression of transcripts that are characteristic of SCLCs and LuSCC lineages[16] (Figure 4E). After filtering, we identified four and 11 acquired alterations in PDC4.2 and PDC5.2, respectively (supplementary Table S8, available at *Annals of Oncology* online), including an *FGFR3—TACC3* fusion in PDC5.2, which is involved in acquired resistance to EGFR-TKIs (supplementary Figure S5D, available at *Annals of Oncology* online). This fusion may explain the LuSCC differentiation features observed in these cells. *MDM2* was also strongly reamplified in PDC5.2, although its involvement in resistance to TKI is unknown (supplementary Figure S5E, available at *Annals of Oncology* online).

Germline mutations in cancer predisposition genes in NSK-LuADs

The somatic mutation at *TP53* found in PDC4 was heterozygous and the inspection of the Integrative Genomics Viewer allowed us to identify another mutation (p.Arg158His) in the germline (DNA from the blood). The mother of patient #4, also diagnosed with LuAD, carried the germline *TP53* mutation, making it consistent with Li—Fraumeni syndrome. Both patients showed *EGFR* mutations in their tumors. This observation prompted us to scrutinize an independent cohort of 27 primary NSK-LuADs to search for cancer predisposition variants. The germline of these patients was examined using WES or direct Sanger sequencing of *TP53*, *BRCA1*, and *BRCA2* (supplementary Table S2, available at *Annals of Oncology* online). Further, we scrutinized WES data from TCGA cohorts and observed changes at dominant and at recessive cancer predisposition genes, affecting 6% of the NSK-LuADs (Table 1). Two changes, the p.Asn588Ser at *BRCA2* and the p.Arg290His at *TP53*, are listed as variant of unknown significance (VUS). In the tumor, the VUS at *TP53* was concomitant with a somatic mutation (p.Cys141Tyr) without loss of heterozygosity. The p.Arg290His variant has been reported to appear somatically in human cancer and to be inactivating.[17] Finally, heterozygous pathogenic mutations were found in the *BLM*, *FANCL*, and *WRN*, associated with the Bloom, Fanconi anemia, and Werner syndromes, respectively, when biallelically inactivated in the germline.

DISCUSSION

This comprehensive analysis of PDCs from NSK-LuADs revealed alterations in well-established non-smoking-associated drivers and novel potential TSGs and oncogenes. ATF7IP, a transcriptional modulator involved in heterochromatin formation, through the stabilization of the histone methyltransferase SETDB1,[18] was found to be inactivated in 5% of the LuADs, making its potential involvement as a TSG worthy of further investigation. Moreover, the *MB21D2* gene, for which there is almost no available information, was found mutated in a hotspot which is of interest and suggests an oncogenic role. *MB21D2* may be related to *MB21D1* which codes for the cyclic guanosine monophosphate—adenosine monophosphate synthase, functionally associated with the immunity-related protein STING.[19]

Our results are firm evidence that *RB1* inactivation is a common event in *EGFR*-mutant LuADs and that ICR is the preferred mechanism. The reasons why *RB1* inactivation is more common in *EGFR*-mutant LuADs than in other type of LuADs, and why the main alteration is ICRs, instead of point mutations, as in SCLC, remain to be ascertained. *EGFR*-mutant tumors may be more prone to double-strand breaks (DSBs) or carry deficiencies in the repair of DSBs. The alterations at *EGFR*, by insertions or deletions at exons 19 and 20, would be consistent with this type of dysfunction.

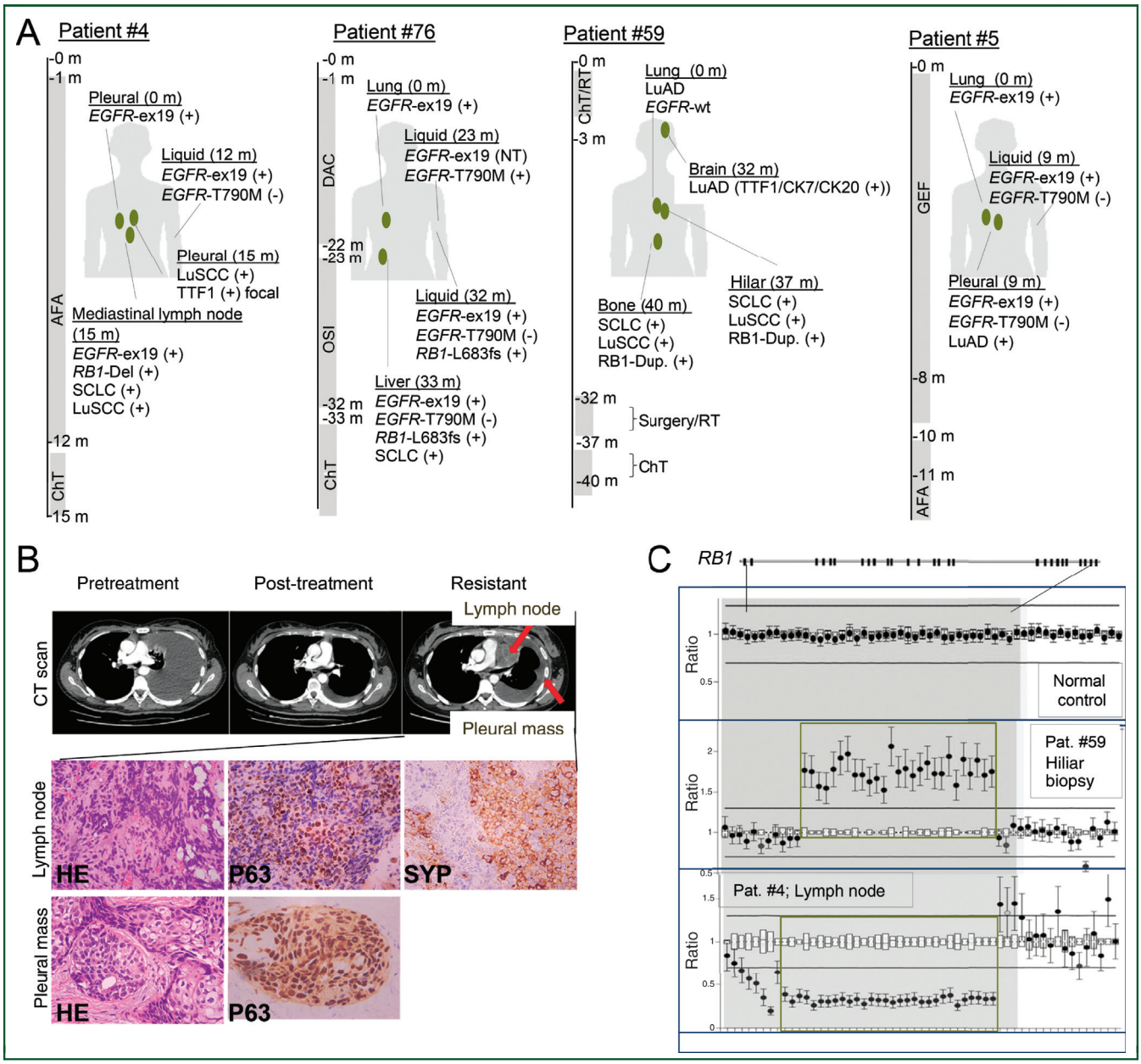

Figure 3. **Dissection of the molecular events underlying SCLC/LuSCC transformation. (A) Treatment received and sample extraction timelines (m, months) for each indicated patient. On the basis of the identification of *EGFR*-mutant tumors, patients were treated with a first-line EGFR-TKI. Patient #4: afatinib (AFA), carboplatin/pemetrexed (ChT); Patient #76: dacomitinib (DAC), osimertinib (OSI), and cisplatin/etoposide (ChT). Patient #59: concurrent chemoradiotherapy (cChT-RT), brain surgery plus radiotherapy (surgery/RT), platinum-based ChT (ChT). Patient #5: gefitinib (GEF) and afatinib (AFA). Genotyping of *EGFR* in patients #4, #5, and #59 and in the liquid biopsy of patient #76 (at 23 months) was performed using the cobas EGFR Mutation Test v2 (Roche Molecular Diagnostics, Basel, Switzerland). *RB1*-mutation at 32 months in patient #76 was found using Guardant360 (Illumina HiSeq, Guardant Health, Redwood City, CA) and the *RB1*-ICR in patients #4 and #59, using multiplex ligation-dependent probe amplification (MLPA). (B) Upper panel: diagnostic computed tomography scan (CT scan) of patient #4. Left, massive left pleural effusion prior to treatment with TKIs (pretreatment); middle, pleural effusion reduction upon TKI treatment (post-treatment); right, disease progression evident from a new lesion suggesting a mediastinal lymph node that extends toward the left pulmonary artery and extensive loculated pleural effusion (resistant). Lower panels: Hematoxylin–eosin (HE) staining and immunostainings of P63 and of synaptophysin (SYP) of the biopsies from the lymph node (mixed LuSCC/SCLC) and pleural mass (LuSCC; 15 months after initial diagnosis) after resistance to the TKI (resistant; magnification, ×400). (C) Upper panel, schematic representation of the structure of *RB1,* with all its corresponding exons. Bottom panels, ratio charts of the MLPA depicting the deletion or duplication of various exons in the indicated biopsies and patients. An appropriate normal control is also included. The rectangle indicates the exons that had suffered duplication and deletion.**

LuAD, lung adenocarcinoma; LuSCC, lung squamous cell carcinoma; SCLC, small-cell lung cancer; TKI, tyrosine kinase inhibitor.

Moreover, we show that the LuAD patients who experienced SCLC/LuSCC transformation after relapse to treatment carried *RB1*-inactivated tumors. The cell of origin of some *EGFR*-mutant LuADs, type II alveolar cells, also has the potential to become SCLC, which may explain their capability to transdifferentiate.[20] Another important question is whether inactivation of *RB1* is involved in the acquired resistance to EGFR-TKI treatment. We found that this alteration could precede the acquisition of resistance to the TKI, and that SCLC/LuSCC transformation can be found concomitantly with the acquisition of the *EGFR-T790M* mutation or the *FGFR3–TACC3* fusion. It was of particular note that an *EGFR*-wild-type LuAD also acquired

https://doi.org/10.1016/j.annonc.2019.09.001

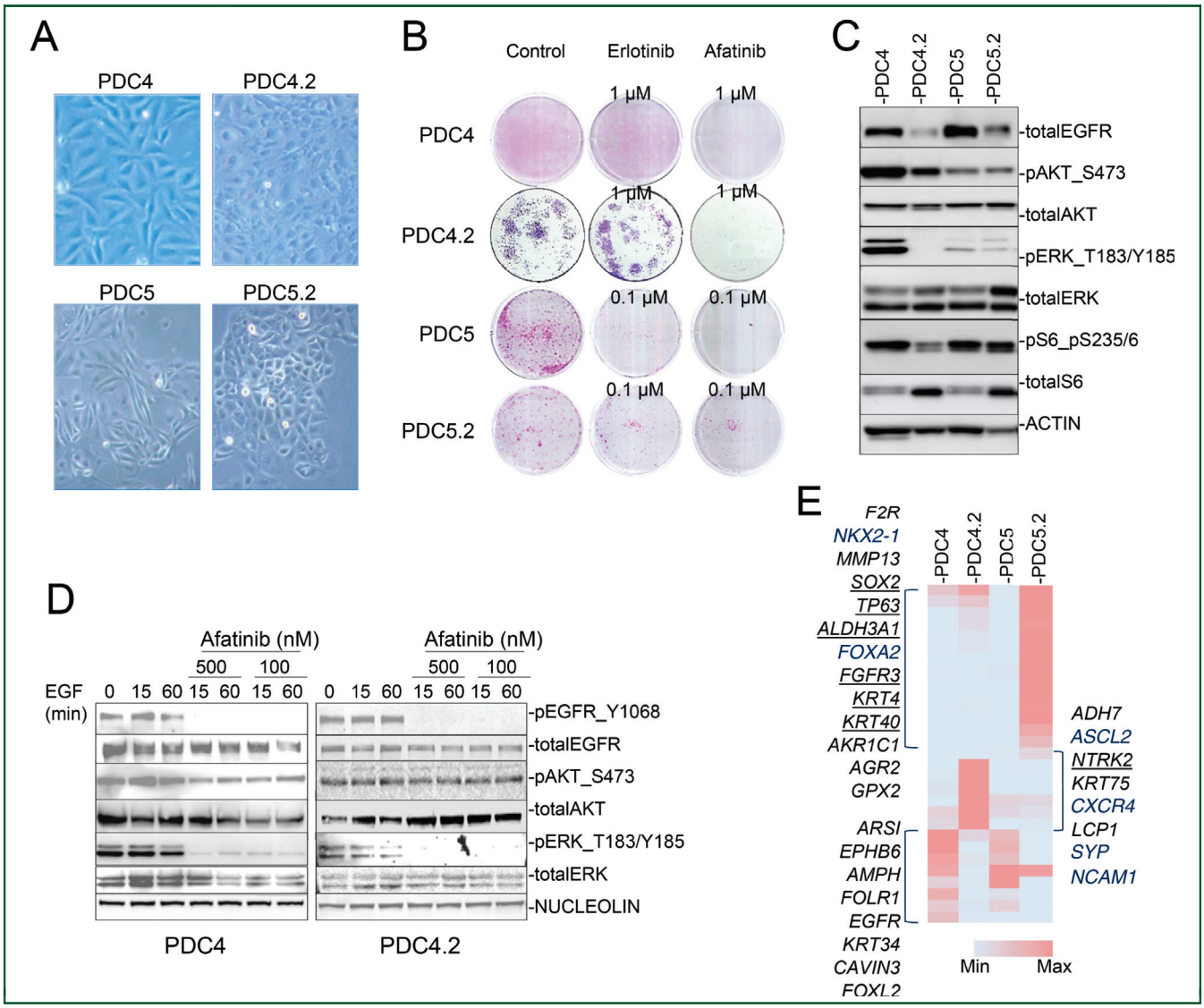

Figure 4. Dissection of the molecular events underlying SCLC/LuSCC transformation during the acquisition of resistance to treatment in LuAD patients. (A) Phase-contrast images of the indicated patient-derived cancer cells (PDCs), showing the changes in cell morphology between the parental and the indicated resistant cells (×200 magnification). (B) Colony-formation assay for each indicated PDCs to show cell-growth inhibition upon administering afatinib or erlotinib at the indicated concentrations. (C) Western blot analysis to show the phosphorylation levels of proteins involved in signal transduction pathways, in the PDC4 and PDC5 cells and in their corresponding cells after acquisition of resistance to EGFR-TKI (PDC4.2 and PDC5.2). ACTIN, protein-loading control. (D) Western blot analysis of the indicated proteins in the PDC4 and PDC4.2 cells, upon treatment with EGF (30 nM) at different times with and without afatinib, at the indicated concentrations. NUCLEOLIN, protein-loading control. (E) Heatmap showing a selection of transcripts that show changes in gene expression, by RNA-seq (normalized counts), in the indicated PDCs from tumors before and after having acquired resistance to EGFR-TKI. Some of these transcripts are characteristic of LuSCC (underlined) or SCLC (in blue). The heatmap was generated with MS Excel (Microsoft, Richmond, WA) conditional formatting based on normalized count values; red indicates the maximum (Max) and light blue the minimum (Min) values.

EGF, epithelial growth factor; LuAD, lung adenocarcinoma; LuSCC, lung squamous cell carcinoma; SCLC, small-cell lung cancer; TKI, tyrosine kinase inhibitor.

SCLC/LuSCC transformation following chemoradiotherapy. Collectively, these observations suggest that the inactivation of *RB1*, *per se,* does not confer resistance to EGFR-TKIs or to standard chemotherapy. Instead, it may favor tumor aggressiveness, by promoting cell plasticity and SCLC/LuSCC transformation under growth-inhibition pressure, thus facilitating the rise of cancer cells with resistance-associated mutations. While the contribution of *RB1* inactivation to the acquired resistance to EGFR-TKIs remains to be fully ascertained, the status of *RB1* in *EGFR*-mutant LuADs, including ICRs, may need to be considered as a marker predicting the risk of LuAD transformation to a more aggressive type of LC.

Finally, we observed that a subset of non-smoking-associated LC patients carries germline heterozygous mutations at autosomal recessive (*BLM*, *FANCL,* and *WRN)* and at dominant cancer-predisposing genes, especially in *TP53*. Although an increased risk of LC in Li—Fraumeni patients has been documented, little is known about the accumulation of *EGFR*-mutant tumors among these patients. Only some case reports have been published in this regard.[21] The possible familiar aggregation of cancer may need to be taken into account in NSK-LuADs patients, in order to identify those individuals who could be offered genetic counseling to evaluate cancer predisposition syndromes.

Table 1. List of changes found in the germline of NSK-LuADs patients at genes that have been associated with cancer predisposition

Case	Age/sex	Other cancer (age)	Germline	Syndrome	Rs (MAF)	Status (Clinvar)	*EGFR* status	*RB1* status in the primary tumor
Patient #4[a]	38/F	NO	*TP53* p.Arg158His	Li–Fraumeni	*rs587782144* (0.00001)	Mutation	Mutant p.Glu746_A750del	Mutant ICR (E3-27)
Patient #61[a]	54/F	NO	*TP53* p.Arg158His	Li–Fraumeni	*rs587782144* (0.00001)	Mutation	Mutant p.Leu858Arg	Mutant ICR (I1)
Patient #13	53/F	NO	*TP53* p.Arg290His	Li–Fraumeni	*rs55819519* (0.00016)	VUS	Mutant p.Leu858Arg	nd
Patient #74	77/F	Uveal melanoma (76 years)	*BRCA2* p.Asn588Ser	Breast–ovarian cancer	*rs373400041* (0.00003)	VUS	Mutant p.Glu746_A750del	nd
Patient #28	73/F	nd	*BLM* p.Arg899Ter	Bloom	*rs587779884* (0.00007)	Mutation (recessive)[b]	Wild type	Wild type
Patient #22	73/F	nd	*FANCL* p.Thr372Asnfs	Fanconi anemia	*rs759217526* (0.0029)	Mutation (recessive)[b]	Wild type	Wild type
TCGA 95.8039	72/M	NO	*BRCA1* p.Leu392Glnfs	Breast–ovarian cancer	*rs80359874* (0.00001)	Mutation	Wild type	nd
TCGA 05.5429	60/M	NO	*CHEK2* p.Ile157Thr	Susceptibility to several cancers	*rs17879961* (0.004)	Mutation	Wild type	nd
TCGA 55.8087	59/F	NO	*WRN* p.Arg987Ter	Werner syndrome	*rs747319628* (0.00002)	Mutation (recessive)[b]	Mutant p.Glu746_Ser752delinsVal	nd

WES data from PDCs ($n = 11$), LuADs primaries ($n = 14$), and from two cohorts of primary tumors from databases (TCGA, $n = 96$; SRP022932, $n = 16$). Targeted sequencing of *TP53*, *BRCA1*, and *BRCA2* in primary LuADs ($n = 13$; supplementary Figure S2, available at *Annals of Oncology* online). All the germline mutations found were heterozygous. The status of the variants was extracted from the ClinVar database (https://www.ncbi.nlm.nih.gov/clinvar/).
F, Female; ICR, intragenic complex rearrangement; M, Male; MAF, minor allele frequency; nd, no data available; NSK-LuAD, non-smoking-related lung adenocarcinoma; PDC, patient-derived cancer cell; TCGA, The Cancer Genome Atlas; VUS, variant of unknown significance; WES, whole-exome sequencing.

[a] Patients from the same family: mother (patient #61) and daughter (patient #4).

[b] Heterozygous pathogenic mutations in recessive genes.

ACKNOWLEDGEMENTS

The authors acknowledge the technical assistance of Isabel Bartolessis, Laia Puig, and Ana Navarro of the Genes and Cancer Group at IDIBELL. We also acknowledge the assistance of the HUB-ICO-IDIBELL and IGTP-HUGTP Biobanks and of the Spanish National Genome Analysis Center (CNAG-CRG, Barcelona, Spain). The RNA-sequencing raw data produced by this study are available at Gene Expression Omnibus (GEO) under the accession code GSE135164.

FUNDING

This work was supported by the Fundacion Cientifica Asociacion Española Contra el Cancer-AECC (grant number GCB14142170MONT) to LMM, MS-C, and EF; the Spanish Ministry of Economy and Competitivity-MINECO (grant number SAF-2017-82186R to MS-C; Rio Hortega-CM17/00180 to MS; PROYBAR17005NADA to EN); the Health Institute Carlos III-ISCIII, Fondo Europeo de Desarrollo Regional-FEDER (grant Number PT13/0001/0044, PT17/0009/0019, PI16 01821); the Government of Navarra (grant number DIANA project); and the Ramon Areces Foundation (no grant number is applicable) to LMM and RP.

DISCLOSURES

EF reports the following conflicts of interest: advisory role or speaker's bureau: AbbVie, AstraZeneca, BerGenBio, Blueprint medicines, Boehringer Ingelheim, Bristol-Myers Squibb, Celgene, Eli Lilly, Guardant Health, Janssen, Medscape, Merck KGaA, Merck Sharp & Dohme, Novartis, Pfizer, priME Oncology, Roche, Samsung, Takeda, Touchtime. Board: Grifols, independent member. Research funding: Fundación Merck Salud, Grant for Oncology Innovation EMD Serono. OJ-V reports the following conflicts of interest: receiving personal fees from Boehringer Ingelheim, BMS, MSD, Roche/Genentech, Astra-Zeneca, Abbvie, outside the submitted work. CL reports the following conflicts of interest: Pfizer IDM Oncology Regional Breast Advisory Board. Teleconference Global Biomarker Expert Input Forum. All other authors have declared no conflicts of interest.

REFERENCES

1. Siegel RL, Miller KD, Jemal A. Cancer statistics, 2018. *CA Cancer J Clin*. 2018;68:7–30.
2. Scagliotti GV, Longo M, Novello S. Nonsmall cell lung cancer in never-smokers. *Curr Opin Oncol*. 2009;21:99–104.
3. Govindan R, Ding L, Griffith M, et al. Genomic landscape of non-small cell lung cancer in smokers and never-smokers. *Cell*. 2012;150:1121–1134.
4. Cancer Genome Atlas Research Network. Comprehensive molecular profiling of lung adenocarcinoma. *Nature*. 2014;511:543–550.
5. Rosell R, Bivona TG, Karachaliou N. Genetics and biomarkers in personalization of lung cancer treatment. *Lancet*. 2013;382:720–731.
6. Blanco R, Iwakawa R, Tang M, et al. A gene-alteration profile of human lung cancer cell lines. *Hum Mutat*. 2009;30:1199–1206.
7. Nahar R, Zhai W, Zhang T, et al. Elucidating the genomic architecture of Asian EGFR-mutant lung adenocarcinoma through multi-region exome sequencing. *Nat Commun*. 2018;9:216.
8. Yu HA, Suzawa K, Jordan E, et al. Concurrent alterations in EGFR-mutant lung cancers associated with resistance to EGFR kinase

inhibitors and characterization of mTOR as a mediator of resistance. *Clin Cancer Res*. 2018;24:3108—3118.
9. Gazdar AF, Girard L, Lockwood WW, et al. Lung cancer cell lines as tools for biomedical discovery and research. *J Natl Cancer Inst*. 2010;102:1310—1321.
10. Oie HK, Russell EK, Carney DN, et al. Cell culture methods for the establishment of the NCI series of lung cancer cell lines. *J Cell Biochem Suppl*. 1996;24:24—31.
11. Pereira C, Gimenez-Xavier P, Pros E, et al. Genomic profiling of patient-derived xenografts for lung cancer identifies B2M inactivation impairing immunorecognition. *Clin Cancer Res*. 2017;23:3203—3213.
12. Chase A, Ernst T, Fiebig A, et al. TFG, a target of chromosome translocations in lymphoma and soft tissue tumors, fuses to GPR128 in healthy individuals. *Haematologica*. 2010;95:20—26.
13. Sondka Z, Bamford S, Cole CG, et al. The COSMIC Cancer Gene Census: describing genetic dysfunction across all human cancers. *Nat Rev Cancer*. 2018;18:696—705.
14. Vogelstein B, Papadopoulos N, Velculescu VE, et al. Cancer genome landscapes. *Science*. 2013;339:1546—1558.
15. Niederst MJ, Sequist LV, Poirier JT, et al. RB loss in resistant EGFR mutant lung adenocarcinomas that transform to SCLC. *Nat Commun*. 2015;6:6377.
16. Angulo B, Suarez-Gauthier A, Lopez-Rios F, et al. Expression signatures in lung cancer reveal a profile for EGFR-mutant tumours and identify selective PIK3CA overexpression by gene amplification. *J Pathol*. 2008;214:347—356.
17. Giacomelli AO, Yang X, Lintner RE, et al. Mutational processes shape the landscape of TP53 mutations in human cancer. *Nat Genet*. 2018;50:1381—1387.
18. Timms RT, Tchasovnikarova IA, Antrobus R, et al. ATF7IP-mediated stabilization of the histone methyltransferase SETDB1 is essential for heterochromatin formation by the HUSH complex. *Cell Rep*. 2016;17:653—659.
19. Ablasser A, Chen ZJ. cGAS in action: expanding roles in immunity and inflammation. *Science*. 2019;363(6431):eaat8657.
20. Oser MG, Niederst MJ, Sequist LV, et al. Transformation from non-small-cell lung cancer to small-cell lung cancer: molecular drivers and cells of origin. *Lancet Oncol*. 2015;16:e165—e172.
21. Ricordel C, Labalette-Tiercin M, Lespagnol A, et al. EFGR-mutant lung adenocarcinoma and Li-Fraumeni syndrome: report of two cases and review of the literature. *Lung Cancer*. 2015;87:80—84.